# Unitarization of the classical statistical *s* matrix for systems with localization

Richard L. Weaver*
*Department of Physics, University of Illinois, 1110 W. Green Street, Urbana, Illinois 61801, USA*
(Received 1 August 2007; published 21 November 2007)

It has recently been observed that a large reverberant cavity admits a classically motivated random *s* matrix that is not unitary but that can be made so in a minimally invasive manner. A random process with an envelope $\langle s^2(t)\rangle \sim \exp(-t/T_H)$ representing reflection from a structure having no internal time scales other than Heisenberg time $T_H$ was shown to lead to a unitary *S* matrix exhibiting mesoscopic behaviors not present in the classically inspired original $\langle s^2(t)\rangle$. These included enhanced backscatter, quantum echo, power law tails, and level repulsion. Here the procedure is extended to two systems having, in addition to Heisenberg times, internal time scales corresponding to conduction and diffusion. The repaired *S* matrices for coupled rooms and one-dimensional random structures with multiple scattering are found to correspond to Wigner *K* matrices with signatures of localization.

DOI: 10.1103/PhysRevE.76.051122 PACS number(s): 05.60.Gg, 05.45.Mt, 11.55.−m

## I. INTRODUCTION

Disordered and irregular wave bearing structures permit statistical particle dynamics models for the evolution of their energy densities. Thermodynamic models of phonon or electron transport in which inelastic scattering is presumed to have destroyed phase coherence of the waves are of this sort. A picture of particles as diffusing in a random potential is both attractive and useful. But in the absence of inelastic scattering, waves preserve phase coherence, so neglect of wave interference is not justified. In such systems mesoscopic features appear which have no classical particle counterpart and are not predicted within the diffusion picture. Amongst these one counts Anderson localization and the associated absence of transport, enhanced backscatter, quantum echo, and power law decays. Each of these behaviors is already understood, more or less well, for simple structures. Anderson localization pertains to infinite statistically homogeneous multiply scattering structures. Power law tails pertain to the time-dependent probability that a quantum particle will remain in a single irregular reverberant cavity before escaping through an open channel. Random matrix theory [1–3] permits the calculation of such probabilities, but its methods are analytically challenging and are correspondingly unlikely to be applied to more general structures.

There exist structures for which no quantitative theory of mesoscopic wave behavior exists. Nevertheless, such structures, even if complicated and statistically inhomogeneous, will usually permit a thermodynamic picture of probability flow based on phase incoherence and inelastic scattering. Statistical energy analysis [4] and its generalizations [5,6] are well known in structural acoustics and vibrations. Electronics in quantum dots and circuits, room acoustics [7,8], diffuse field ultrasonics [9–11], and optical radiative transfer provide other examples. All of these subjects permit a statistical particle picture, valid we presume in the presence of sufficient inelastic scattering, but which is incorrect if phase coherence is retained.

A recent report [12] proposed an ad hoc recipe for repairing a classical statistical particle theory of probability flow. The method was applied to waves reflecting from an irregular structure lacking any internal time scales except level density. It produced probability flows with mesoscopic features remarkably similar to those obtained by averaging over Gaussian orthogonal ensembles of random matrices [1–3].

Here we report application of the recipe to systems having additional transport time scales and for which localization is expected. Probability flow envelopes $E(t)$ are first obtained by arguments predicated on classical diffusion and escape. $\sqrt{E}$ is then multiplied by uncorrelated Gaussian random numbers to produce a classical random *s* matrix $s(t)$, a function that represents a plausible reflected wave amplitude from a complex system with random scattering and phase incoherence. As noted previously [12] this is unlikely to be unitary, and is thus inadmissible as a true *s* matrix. That such an $s(t)$ is unlikely to be unitary is evident, as the trajectories implicit in its construction will have no special phase relations. Even in semiclassical methods, where trajectories are examined in detail, it is difficult [13] to account for all coherences between different orbits.

The recipe continues by invoking a unitarization procedure that produces a unitary $S(t)$ from $s(t)$, a procedure designed to be minimally invasive and to respect the classical flow in $s(t)$ to the extent possible. The repaired *S* matrices are found as previously [12] to exhibit enhanced backscatter and power law tails. The transport of wave intensity in the corresponding closed systems is then constructed from *S*, and examined for signs of localization. In all cases we find that the resulting wave dynamics in the closed system exhibits signs of localization to the extent expected. This is perhaps unsurprising. If a structure is such that most trajectories beginning at the incoming channel then escape back through that channel before much transport has occurred, then the reflection $S(t)$ contains no record of transport. Because responses in the corresponding closed system are concatenations of *S* they also will have little signature of transport, hence the localization seen in the closed systems.

Two classes of structures are studied, each with a range of parameters. Section III considers a pair of coupled reverber-

*r-weaver@uiuc.edu

 

ant cavities with a single $s$-matrix channel attached to one cavity. When closed, and when coupling between them is slow compared to the inverse of the Heisenberg times of the rooms, $T_H = 2\pi\partial$ mode count$/\partial\omega$, such systems are known to exhibit what one might term "Thouless localization" [14,15]. Section IV considers a finite one-dimensional medium whose classical particle dynamics is diffusive. A single channel is attached at the center. Waves in closed versions of such structures are known to be Anderson localized with a localization length of the order of the bare diffusivity divided by the density of states.

## II. MATHEMATICAL PRELIMINARIES

The following section reviews definitions and relationships among scattering matrices, Wigner reaction matrices, Green's functions, and Hamiltonians for a classical wave system. The procedure by which a nonunitary $s$ matrix for a discrete time domain $s_t$ may be filtered in a minimally invasive manner to return a unitary $S_t$ is described in Sec. II B. Finally, an exact relation is recalled between the $S$ matrix of an open system and the internal dynamics of the closed system as represented by its Green's function. These methods and relations are then applied in Secs. III and IV.

### A. Green's functions and scattering matrices for a classical wave field

We begin with the governing equations for a classical wave in a finite discrete domain under the influence of a source $q(t)$ and dissipation.

$$\partial_t^2\{\psi(t)\} = -[H]\{\psi(t)\} - [C]\partial_t\{\psi(t)\} + \{q(t)\}. \tag{1}$$

The $\mathcal{N}\times\mathcal{N}$ symmetric real matrices $[H]$ and $[C]$ are stiffness and damping matrices, respectively. $C$ is positive semidefinite and can in principle have (even) frequency dependence. The $\mathcal{N}$-component vector $\{\psi(t)\}$ is the wave field. The damping matrix may be written in its orthonormal spectral decomposition

$$[C] = \sum_{c=1}^{M} \chi_c\{v_c\}\{v_c\}^T \tag{2}$$

in terms of real positive semidefinite $\chi$ and a set of $M$ mutually orthonormal real vectors $\{v\}$, each with $N$ components. The series may sometimes be truncated at a number of channels $M \ll \mathcal{N}$.

Equation (1) corresponds to an $\mathcal{N}\times\mathcal{N}$ Green's function

$$\partial_t^2[G(t)] + C\partial_t[G(t)] + [H][G(t)] = \delta(t)[I], \tag{3}$$

which has a version without damping

$$\partial_t^2[G^0(t)] + [H][G^0(t)] = \delta(t)[I]. \tag{4}$$

These have Fourier transforms

$$[\tilde{G}(\omega)] = \int_0^\infty [G(t)]\exp(-i\omega t)dt = [H - \omega^2 + i\omega C]^{-1}, \tag{5}$$

and

$$[\tilde{G}^0(\omega)] = \int_0^\infty [G^0(t)]\exp(-i\omega t)dt = [H - (\omega - i\varepsilon)^2]^{-1}. \tag{6}$$

Often the $\{v\}$ can be identified with open waveguides through which wave energy can be carried out. Conversely, a channel can also carry waves into the structure, where they reverberate and then escape, either through a different channel (transmission) or back through the original (reflection). An $M\times M$ scattering matrix $\mathsf{S}$ amongst these channels is defined by

$$\mathsf{S}_{ab}(\omega) = \delta_{ab} - 2i\omega\{v_a\}^T\sqrt{\chi_a}[\tilde{G}(\omega)]\{v_b\}\sqrt{\chi_b}. \tag{7}$$

There is a factor $\omega$ in the second term here, not present for the Schrödinger equation [1,2,16]. We also define the (real except at resonances) symmetric $M\times M$ Wigner reaction matrix $\mathsf{K}$,

$$\mathsf{K}_{ab}(\omega) = \sqrt{\chi_a\chi_b}\{v_a\}^T[\tilde{G}^0(\omega)]\{v_b\}. \tag{8}$$

Except for the factors of $\sqrt{\chi}$ this is the (Fourier transform of the) response of the closed system $[G^0(t)]$ as evaluated at $\{v_a\}$, due to a source $\{v_b\}\delta(t)$.

We deduce

$$\mathsf{S}(\omega) = \mathsf{I} - 2i\omega\mathsf{K}/(\mathsf{I} + i\omega\mathsf{K}) = (\mathsf{I} - i\omega\mathsf{K})/(\mathsf{I} + i\omega\mathsf{K}), \tag{9}$$

which is manifestly unitary. $\mathsf{K}$ is given in terms of $\mathsf{S}$ by

$$\mathsf{K}(\omega) = \mathsf{I}/i\omega - (2/i\omega)\mathsf{S}/(1+\mathsf{S}) = \frac{1}{i\omega}[\mathsf{I} - 2\mathsf{S} + 2\mathsf{S}^2 - 2\mathsf{S}^3 \ldots]. \tag{10}$$

Equations (10) and (8) permit one to determine the response $G^0$ of the closed system from knowledge of $\mathsf{S}$ and the $\chi$. In particular, we note that the reverberant part of $-\partial_t K_{bb}/2$ (the part without the singularity at $t=0$) is, by Eq. (10), $S/(1+S)$. It is also, by Eq. (8), the reverberant part of the diagonal $bb$ element of $(\chi_b/2)[\partial_t G^0]$.

### B. Repair algorithm

In [12], and in Secs. III and IV below, numerical experiments are begun by generating plausible random reflected wave amplitudes $s(t)$ from complex systems in which waves scatter and incur phase incoherence. Such functions are unlikely to be unitary and are therefore inadmissible as $s$ matrices for phase coherent scattering. A unitarization procedure is then applied, designed to be minimally invasive and to respect the classical picture to the extent possible. The details of that procedure are described below.

In the examples studied here, time $t$ is discrete, and runs from 1 to $N$, where $N$ varies with the test but is usually of order $2^{21-23}$, much greater than the time scales for energy flow (e.g., Heisenberg times for recapture), which are in turn taken to be much greater than unity. For the technical reasons described below we choose $N$ large enough that $s_t$ is negligible for $t > N/2$ and then set $s_t$ to zero for those $t$. If the time domain were infinite, $N=\infty$ (while remaining discrete), a nonunitary $s_t$ may be repaired by convolving it with the

causal real minimum phase function $h_t$ whose Fourier transform is given exactly by

$$\tilde{h}(\omega) = \exp\{\tilde{a}(\omega)\} = \exp\{(1/\pi)\sum_{t=0}^{\infty}(1-\delta_{t0}/2)\ \exp(-i\omega t)$$
$$\times\left[\int_{-\pi}^{\pi}\exp(i\alpha t)(-\ln|\tilde{s}(\alpha)|)d\alpha\right], \quad (11)$$

where

$$\tilde{f}(\alpha) = \sum_{t=-\infty}^{\infty} f_t \exp(-i\alpha t), \quad f_t = \frac{1}{2\pi}\int_{-\pi}^{\pi}\tilde{f}(\omega)\exp(i\omega t)d\omega \quad (12)$$

define the Fourier transform pair appropriate for discrete infinite time. Inspection shows that $h$ is causal and minimum phase (because it is the exponentiation of an explicitly causal function $a$ and is therefore analytic and without zeros in the lower half plane). Further scrutiny shows that its spectrum satisfies $|h(\omega)|=1/|s(\omega)|$. This repair procedure is an exact analytic recipe to repair $s$ and return an $S(\omega)=s(\omega)h(\omega)$, with the (unique up to a constant phase) filter that makes $S$ unitary $|S(\omega)|=1$, and is both causal and minimum phase. The procedure may be described as respecting the time-domain features in $s$ to the maximum extent possible [17].

In practice we cannot integrate over the continuum from $-\pi$ to $\pi$, nor sum over an infinite number of discrete times $t$. The literature on spectral factorization [17,18] suggests a number of practical procedures for constructing $h$. The simplest is perhaps to, in lieu of Eqs. (11) and (12), restrict to a finite time interval and construct

$$\tilde{a}_f = \sum_{t=1}^{N}\exp[2i\pi(f-1)(t-1)/N]\frac{2\Theta_t}{N}$$
$$\times\sum_{f'=1}^{N}\exp[-2i\pi(f'-1)(t-1)/N][-\ln|\tilde{s}_{f'}|], \quad (13)$$

where the discrete Fourier transform pair is defined by

$$\tilde{B}_f = \sum_{t=1}^{N}\exp[2i\pi(f-1)(t-1)/N]B_t,$$

$$B_t = \frac{1}{N}\sum_{f=1}^{N}\exp[-2i\pi(f-1)(t-1)/N]\tilde{B}_f, \quad (14)$$

and can be effected by a fast Fourier transform algorithm. The quantity $\Theta$ is a causality enforcer.

$$\Theta_t = 1/2 \quad \text{for } t=1,$$

$$\Theta_t = 1 \quad \text{for } 1 < t \le N/2,$$

$$\Theta_t = 1/2 \quad \text{for } t = N/2+1,$$

$$\Theta_t = 0 \quad \text{otherwise.} \quad (15)$$

With this definition of $\Theta$ it may be shown that $\mathrm{Re}\,\tilde{a}_f = -\ln|\tilde{s}_f|$.

The repaired $S$ matrix is, in the frequency domain,

$$\tilde{S}_f = \tilde{s}_f \exp(\tilde{a}_f). \quad (16)$$

The approximation to a finite time interval introduces an error. We estimate the degree of error by examining the function $\tilde{g}_f = 1/\tilde{h}_f = \exp(-\tilde{a}_f)$ in the time domain. This function has, if evaluated according to Eq. (11), the same domain of support as $s$, that is, it should vanish for times greater than $N/2$ [17,18]. This condition is used to motivate a choice of array length. $N$ is chosen sufficiently large that the energy in $g$ at times less than $N/2$, $(\Sigma_{t=1}^{N/2} g_t^2)$ is greater than that elsewhere $(\Sigma_{t=N/2+1}^{t=N} g_t^2)$ by a factor close to or greater than $10^6$.

### C. Construction of the Green's function $G^0$ for the closed system

From the above expressions for $\mathsf{K}$ and $G^0$ we derive an expression for the $bb$ element of $-\partial_t G^0$ as $-i\omega \mathsf{K}_{bb}/\chi$. Dropping the term $I$ as uninteresting and having support only at $t=0$, and taking a time derivative, we find that the Fourier transform of $-\partial_t G^0$ is $(2/\chi)S/(1+S)$. As $S$ is unitary, this will have poles wherever $S$'s phase is $\pi$. There is a numerical challenge in negotiating the poles while doing the inverse Fourier transform needed to obtain $S/(1+S)$ in the time domain. (The value of $\chi$ pertaining to 100% prompt transmission is 2, as shown in the Appendix.) The challenge may be met by the simple expedient of multiplying $S_t$ by an artificial decay $\exp(-\beta t)$, taking its Fourier transform, then constructing $S/(1+S)$, taking its inverse Fourier transform, and then multiplying by $\exp(\beta t)$. This procedure is analytically exact for any positive $\beta$. It moves the poles off the real $\omega$ axis, at the cost of losing numerical precision at late times. Squaring $-\partial_t G^0$ then gives energy density at $b$ due to a source at $b$.

In the following sections we introduce what may be called the Sabine reflection coefficient $s_t$ for coupled rooms (Sec. III) and for one-dimensional diffusing media (Sec. IV). The repair procedure described above is then applied to it. The resulting $S_t$'s are examined for mesoscopic signatures. They are also used to derive $-\partial_t K_t/2$'s whose squares can then be compared with Sabine predictions for energy density in closed systems.

## III. CONDUCTION AND LOCALIZATION BETWEEN TWO COUPLED ROOMS

Consider the system pictured in Fig. 1 consisting of two reverberant cavities, each with randomizing, perhaps chaotic, ray dynamics. A single channel is attached to cavity number one, with a prompt transmission coefficient of 100%. The two cavities are coupled through a small window. A room acoustic [7,8] or SEA [4–6] or thermodynamic description of the spectral energy densities $E$ (energy per frequency interval) in each room is given by the coupled differential equations

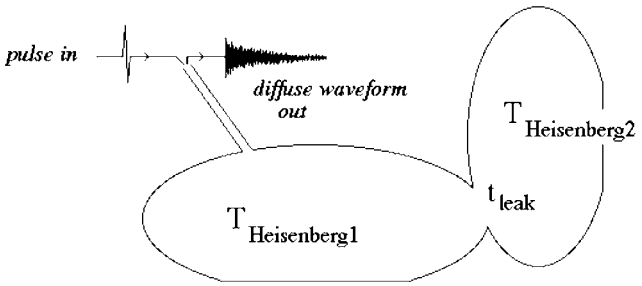


FIG. 1. Two reverberant cavities are weakly coupled through a small window. A single channel through which an ingoing pulse returns a diffuse reflection $s(t)$ is attached to one of the cavities.

$$dE_1/dt = \eta[E_2/n_2 - E_1/n_1] - \sigma E_1 + \delta(t),$$

$$dE_2/dt = \eta[E_1/n_1 - E_2/n_2], \tag{17}$$

where $\eta$ is a (dimensionless) conductance between the rooms. These equations could also be thought of as describing the probability density evolution of a classical particle. It is convenient to identify a "leak time" from room one to room two as $t_{\text{leak}}=n_1/\eta$. $n_1$ and $n_2$ are the spectral densities of the modes, that is, the Heisenberg times, in each room; $n_j=T_{Hj}$. The quantity $\sigma E_1$ represents the rate of energy recapture by the open channel. It may be shown that all the energy originally deposited is recaptured.

$$\sigma \int_0^\infty E_1 dt = 1. \tag{18}$$

The channel has a recapture rate $\sigma$ limited by a thermodynamic argument: $\sigma \leq 1/T_H$ [2,3]. This is an equality, $\sigma = 1/T_{H1} = 1/n_1$, for the assumed 100% transmission.

We take equal sized rooms $n_1=n_2$ and perfect coupling of the channel, $\sigma=1/n_1$, and obtain

$$\frac{d}{dt}\begin{Bmatrix} E_1 \\ E_2 \end{Bmatrix} = \begin{bmatrix} -\sigma-\sigma\eta & \sigma\eta \\ \sigma\eta & -\sigma\eta \end{bmatrix}\begin{Bmatrix} E_1 \\ E_2 \end{Bmatrix} + \begin{Bmatrix} \delta(t) \\ 0 \end{Bmatrix}. \tag{19}$$

This matrix has eigenvalues $\lambda_{1,2}=-\sigma/2[1+2\eta \pm \sqrt{(1+4\eta^2)}]$. The solution of the differential equation is

$$\begin{Bmatrix} E_1 \\ E_2 \end{Bmatrix} = \frac{\sigma}{\eta(\lambda_2-\lambda_1)}\left[(1+\eta+\lambda_2/\sigma)\begin{Bmatrix} \eta \\ 1+\eta+\lambda_1/\sigma \end{Bmatrix}\exp(\lambda_1 t) - (1+\eta+\lambda_1/\sigma)\begin{Bmatrix} \eta \\ 1+\eta+\lambda_2/\sigma \end{Bmatrix}\exp(\lambda_2 t)\right]. \tag{20}$$

The Sabine $s$ matrix is constructed by $s_t=r_t\,[\sigma E_1(t)]^{1/2}$, where $r_t$ is an uncorrelated Gaussian random number, $\langle r\rangle = 0$, $\langle r_t r_{t'}\rangle = \delta_{tt'}$. This $s_t$ is a plausible wave reflection amplitude if internal scatterings are inelastic. Inasmuch as it lacks anything resembling an initial delta function $\delta(t)$, it corresponds to scattering with no prompt reflections, in other words to a channel coupled to the scattering region with 100% prompt transmission. It would in principle be possible to add a prompt reflection $P\delta_{t0}$ to $s_t$, choose a corresponding recapture rate $\sigma$ less than $1/T_H$, and decrease the strength of the later diffuse envelope (it would then be called a "coda") by an amount calculated to retain probability conservation.

Closely associated with the envelope $E_1$ for the Sabine $s$ matrix is the corresponding envelope if recapture is eliminated. In this case Eq. (19) becomes

$$\frac{d}{dt}\begin{Bmatrix} F_1 \\ F_2 \end{Bmatrix} = \begin{bmatrix} -\sigma\eta & \sigma\eta \\ \sigma\eta & -\sigma\eta \end{bmatrix}\begin{Bmatrix} F_1 \\ F_2 \end{Bmatrix} + \begin{Bmatrix} \delta(t) \\ 0 \end{Bmatrix}. \tag{21}$$

Thus

$$F_1(t) = (1/2)[1+\exp(-2\sigma\eta t)], \tag{22}$$

which represents the spectral energy density in the first room subsequent to a unit deposit in that same room when the channel is closed. Equipartition is apparent at $t \gg 1/\sigma\eta$, at which time the energy densities in the two rooms are the same, $F_1=F_2=1/2$. An additional factor of $\sigma$ converts $F_1$ to something that can be compared with $S_t^2$. We note that $\sigma E_1 = \langle s_t^2\rangle \leq \sigma F_1$. The inequality is an equality at times $t \ll 1/\sigma$ before much recapture.

We consider three cases of the two-room structure. Case $A$, whose results are shown in Fig. 2, is a system in which each room has a Heisenberg time $T_H=2000$, and for which the leaking is rapid: $t_{\text{leak}}=T_H/\eta=200$. The dimensionless conductance parameter $\eta$ is 10, much greater than unity, so no localization is expected. The structure should behave like a single room of volume twice that of either room separately. The time-domain arrays were taken with length $N=2^{20}$. An exact procedure following Eq. (11) would produce a repairing filter $h$ having an inverse, which vanishes for times greater than $N/2$. The use of Eq. (13) did not produce such a filter, but the inverse's energy at such times was less than its energy at early times by a factor of 740 000, so the inexactness is judged to be negligible. Figures 2(a) and 2(b) show the behavior of smoothed squared $s_t$ [whose expectation is $\sigma E_1(t)$] and smoothed squared $S_t$. We note, in particular, the power law tail in $\langle S^2(t)\rangle$. At late times $\langle s^2(t)\rangle$ diminishes exponentially like $\exp(\lambda_1 t)$ while $\langle S^2(t)\rangle$ diminishes like $t^{-5/2}$. An enhancement at time zero by a factor of about two may also be seen.

Figures 2(c) and 2(d) show the reverberant part of the smoothed square of the inverse Fourier transform of the resulting $-i\omega G^0 = S(\omega)/[1+S(\omega)]$. This represents twice the kinetic energy density (i.e., the total energy density) of the closed system at the position of the channel subsequent to a unit source at the same position. This may be compared to the Sabine prediction $\sigma F_1$. The energy density in $G^0$ is seen to be greater than it is in $\sigma F_1$, by a factor of 2 at early times and a factor of 3 at late times. These factors are predicted independently in random matrix theory [1,2,16] and termed enhanced backscatter and quantum echo [19]. The behavior here is consistent with that seen previously [12] for a single room; it shows no sign of localization.

In Fig. 3 we consider an intermediate case ($B$) in which each room has a Heisenberg time of 2000, and a leak time of 4000, so dimensionless conductance $\eta=0.5$. The Sabine $\langle s^2(t)\rangle = \sigma E_1$ with its two decay rates $\lambda_{1,2}$ $(=-1/6828, -1/1171)$ may be discerned in the dashed line in Figs. 3(a) and 3(b). The repair process has again augmented $s^2(t)$ with what looks like an enhanced backscatter factor of two at short times in $\langle S_t^2\rangle$ (solid line). Figure 3(c) shows the result-

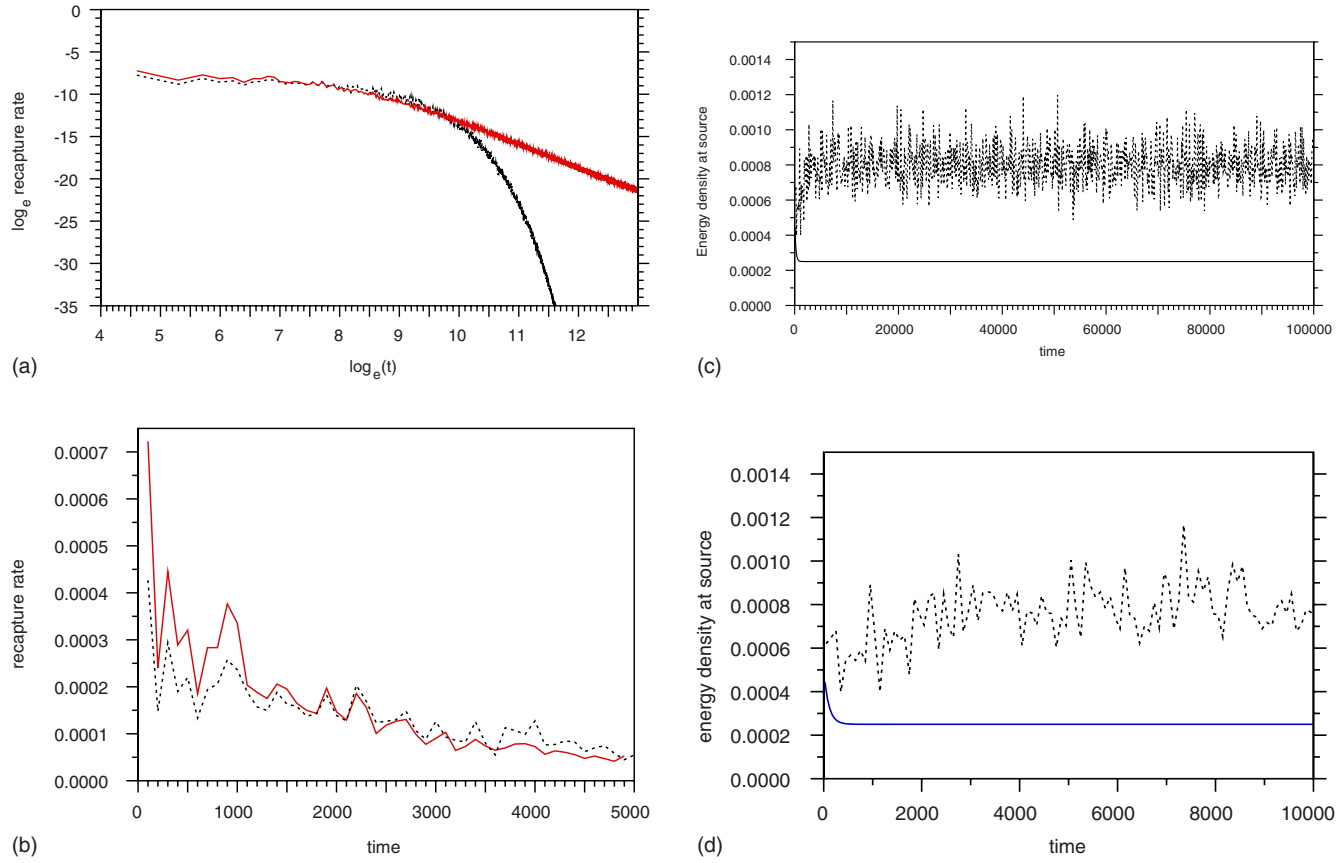


FIG. 2. (Color online) (a) A comparison of the squared and smoothed incoherent Sabine reflection $\langle s^2(t)\rangle$ (dashed line) and the repaired $S$ matrix $\langle S^2(t)\rangle$ [paler (red online) solid line] for case $A$. The rooms are well coupled ($\eta=10$, $T_H=2000$) and behave together like one large room. A power law tail $\langle S^2(t)\rangle \sim t^{-5/2}$ is visible at late times. (b) The enhanced backscatter factor of 2 is seen in this closeup of the data of (a). The repair has reproduced the fluctuations in the original. (c) Case $A$ continued. The reverberant part of $[-\partial_t K(t)/2]$ =reverberant part of $\partial G^0/dt$, i.e., the part without the delta function at time zero, $S/(1+S)$, is squared and smoothed (dashed line) and compared with the Sabine-type prediction $\sigma F_1(t)$ (solid line). An enhanced backscatter factor of 2 is noticeable at early times. A quantum echo appears later in which the enhancement grows to three. As predicted in random matrix theory [19] the quantum echo arrives on a time scale comparable to the effective Heisenberg time, 4000. (d) A closeup of the short time behavior of (c) shows the enhanced backscatter factors. The Sabine $\sigma F_1$ (solid line) shows the leaking process as probability flows from the first room into the second on a time scale of $t_{\text{leak}}=200$.

ing smoothed squared $-\partial_t K(t)/2$ and compares it with $\sigma F_1$. Quantum echo is less apparent than it is in Figs. 2(c) and 2(d), as loss of energy density due to leaking competes with enhancement due to quantum echo.

Late time energy density in room one is greater than is predicted by equipartition. At such times $(\partial_t K/2)^2$ is greater than $\sigma F_1$ by a factor of about 4.4, three parts of which may be attributed to quantum echo. The remainder is localization.

Finally, we consider system $C$, for which localization ought to be more significant. Figure 4 shows the results from a choice $T_H=2000$ for each room, and a leaking time of 25 000 for an $\eta=0.08$. $N$ was taken at $2^{21}$. The presence of two decay rates $\lambda_{1,2}$ is readily seen in the Sabine $\langle s^2(t)\rangle$ shown in Fig. 4(a). Again the repaired $\langle S^2(t)\rangle$ shows an enhanced backscatter factor of two at short times. Figure 4(b) shows that the late time enhancement is stronger (now a factor of about 5.2) than it was in Figure 3, close to the theoretical maximum of 6. Localization is stronger.

In the limit of weak coupling there are analytic predictions for the enhancement at late times. Weaver and Lobkis [14] derived an expression for the fraction of the total energy in room two at late times $e=(\sigma\eta T_H/2\pi)^{1/2}$ or $e=(\sigma\eta T_H/\pi^2)^{1/2}$ depending on the model for the statistics of the coupling. These predictions correspond to an asymptotic enhancement here of $6(1-e)=5.32$ and 5.46, respectively.

In summary, application of the unitarization procedure to construct $S$ matrices for three cases of coupled reverberant cavities have all reproduced the expected mesoscopic energy flows. In particular, the resulting $S(t)^2$ and $(\partial_t G^0)^2$ show enhanced backscatter, quantum echo, power law tails, and Thouless localization.

## IV. DIFFUSION AND LOCALIZATION IN ONE DIMENSION

Consider the system pictured in Fig. 5. A single channel is attached at the center of a length $2L$ quasi-one-dimensional medium with multiple scattering. A classical particle is emitted at $x=0$, diffuses, and is recaptured at $x=0$ according to the PDE and boundary conditions as follows:

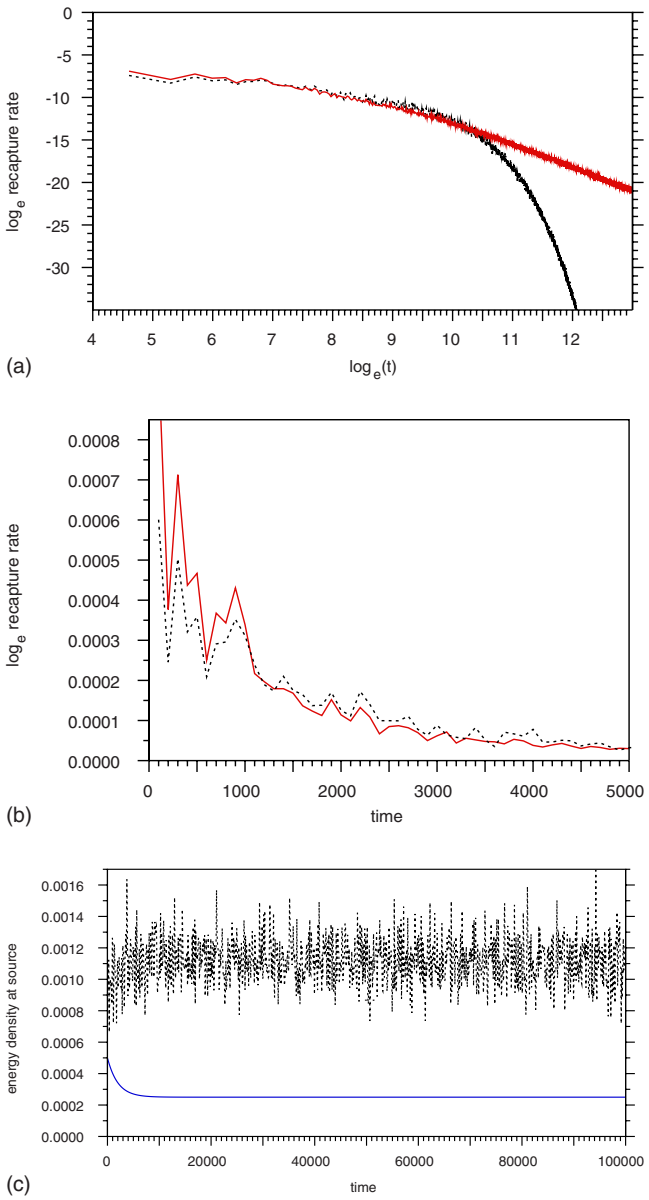


FIG. 3. (Color online) (a) A comparison of the squared and smoothed incoherent Sabine reflection $\langle s^2(t)\rangle$ (dashed line) and the repaired $S$ matrix $\langle S^2(t)\rangle$[paler (red online) solid line] for case $B$ for which the rooms are moderately coupled ($\eta$=0.5, $T_H$=2000). (b) The behavior of the Sabine (dashed line) and repaired recapture rates (solid line) for case $B$ at early time. As in Fig. 2(b) one observes enhanced backscatter and reproduction in $S$ of the fluctuations in $s$. (c) The Sabine $\sigma F_1$ for case $B$ (solid line) shows the relaxation of room one's energy density on the scale of the leak time as energy flows into the second room. The repaired $S$ matrix corresponds to an energy density (dashed line) at the source with a very different behavior. At late times it is enhanced over the Sabine prediction by a factor of 4.4.

$$\partial_t E(x,t) - D\nabla^2 E(x,t) + \sigma\delta(x)E(x,t) = \delta(x)\delta(t),$$

$$\partial_x E(x,t)\,_{x=\pm L} = 0, \tag{23}$$

where $E(x,t)$ is probability (energy for classical waves) density and $\sigma$ is a rate of probability recapture, equal if the coupling is 100%, to the inverse of the density of states; $\sigma = 2L/T_H$. This equation is Laplace transformed to obtain

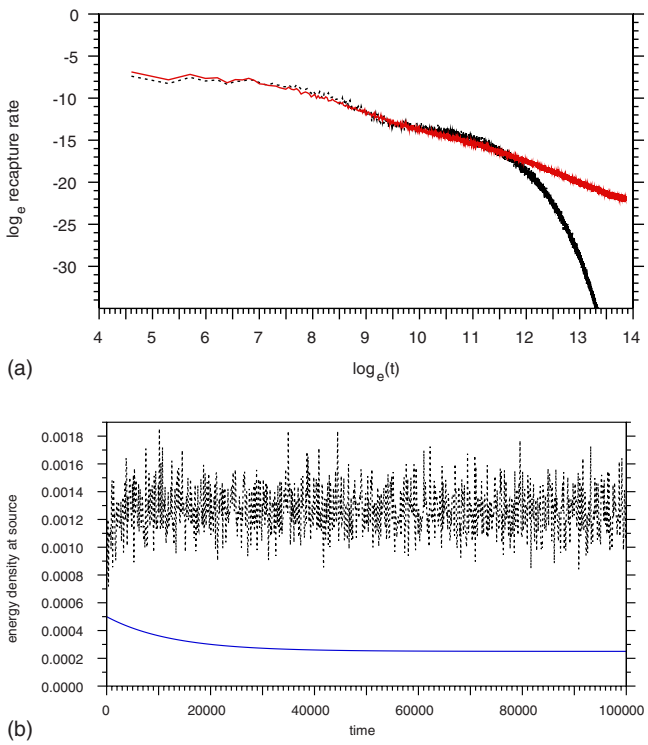


FIG. 4. (Color online) (a) The smoothed squares of the Sabine $s(t)$ (dashed line) and the repaired $S(t)$ [pale solid line (red online)] are compared for the case $C$, for which the cavities are weakly coupled. (b) The Sabine $\sigma F_1$ (solid line) for case $C$ shows the slow relaxation of room one's energy on the scale of the leak time as energy flows into the second room. The repaired $S$ matrix corresponds to an energy density at the source with a very different behavior. At late times it is enhanced over the Sabine prediction by a factor of 5.2.

$$p\bar{E}(x,p) - D\nabla^2\bar{E}(x,p) + \sigma\delta(x)\bar{E}(0,p) = \delta(x),$$

$$\partial_x\bar{E}(x,p)|_{x=\pm L} = 0, \tag{24}$$

which has solution at points other than $x=0$ in the form

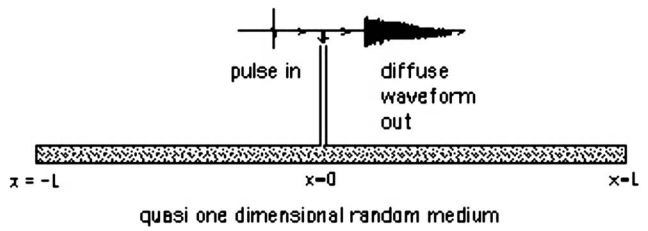


FIG. 5. A single channel is attached to the midpoint of a finite one-dimensional diffusing medium. An ingoing pulse reflects diffusely.

$$\bar{E}(x,p) = A(p)[\exp\{-\sqrt{p/D}|x|\} + \exp\{\sqrt{p/D}(|x| - 2L)\}]. \tag{25}$$

$A(p)$ is determined by integrating the ODE (24) over an infinitesimal region around $x=0$,

$$-2D\partial_x \bar{E}(x,p)|_{x=0+} + \sigma\bar{E}(0,p) = 1, \tag{26}$$

which implies

$$A(p) = [\sigma\{1 + e^{-2L\sqrt{p/D}}\} + 2\sqrt{Dp}\{1 - e^{-2L\sqrt{p/D}}\}]^{-1}. \tag{27}$$

Thus the Laplace transform of the rate of return $\sigma E(0,t)$ is

$$\sigma\bar{E}(0,p) = \sigma[\sigma + 2\sqrt{Dp}\{\tanh 2L\sqrt{p/D}\}]^{-1}, \tag{28}$$

which is one at $p=0$, indicating that $\sigma E(0,t)$ integrates to unity. All probability is recaptured.

$E(0,t)$ is recovered by inverse Laplace transform. Evaluation as a sum over the residues along the negative real $p$ axis gives

$$E(x=0,t) = (1/L)\sum_{m=1}^{\infty} \exp[-\gamma_m^2(t/T)]/[1 + \gamma_m^{-2}(\Xi + \Xi^2)], \tag{29}$$

where $T=L^2/D$ is a classical diffusion time and $\Xi$ is the ratio of classical diffusion time $T$ to Heisenberg time, $\Xi = \sigma L/2D = \sigma T/2L$. As localization length in one dimension is of the order of $2D/\sigma$, $\Xi$ represents the ratio of system size to localization length and therefore serves as a measure of the importance of localization. The $\gamma_m$ are the positive roots of $\gamma \tan \gamma = \Xi$. This series converges quickly at large enough times $t$.

For early times we may approximate $L$ as infinite, and replace the hyperbolic tangent with unity; in this case the poles reduce to a branch cut along the negative real axis. The result is

$$E(x=0,t) = \frac{\sigma}{4\pi D}[\pi^{1/2}\tau^{-1/2} - \pi e^{\tau}\mathrm{erfc}(\sqrt{\tau})], \tag{30}$$

where $\tau = t\sigma^2/4D$ is a dimensionless time.

We also interest ourselves in the Sabine prediction for probability density in the absence of recapture.

$$\partial_t F(x,t) - D\nabla^2 F(x,t) = \delta(x)\delta(t), \quad \partial_x F(x,t)|_{x=\pm L} = 0. \tag{31}$$

This is a conventional diffusion equation; the solution is well known. It may be expressed as a sum over the normal modes of the finite structure. The probability density at $x=0$ is

$$F(0,t) = 1/2L + (1/L)\sum_{n=1}^{\infty} \exp(-n^2\pi^2 Dt/L^2), \tag{32}$$

a series that converges best at late times. (This expression permits us to ascertain the meaning of the time scale $T$ by noting that $T/\pi^2 = L^2/D\pi^2$ is the time at which the diminishing $F(0,t)$ is still 1.55 times the value it takes at $t=\infty$.) $F$ may also be expressed as a sum over diffusive waves from the source and from all image sources at $x = \pm 2nL$.

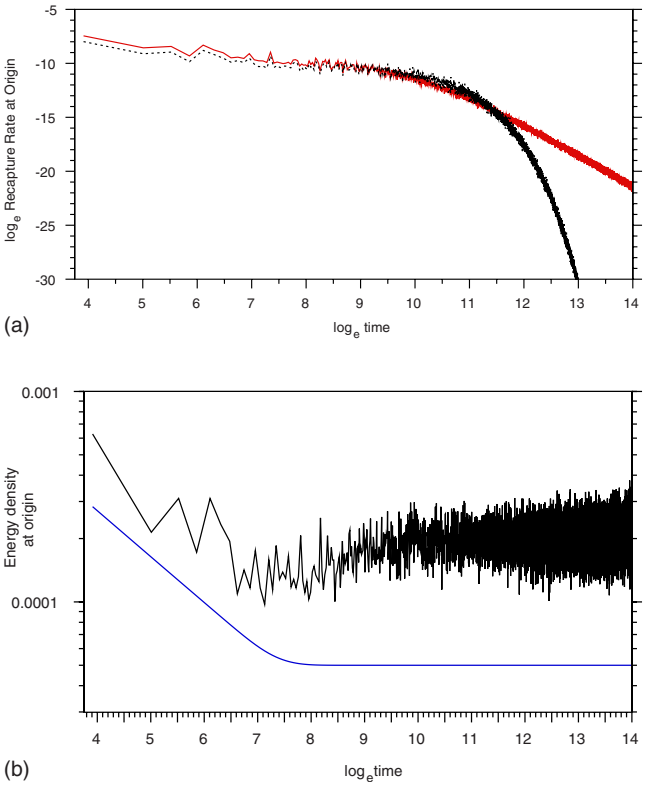


FIG. 6. (Color online) (a) The Sabine envelope $\sqrt{\sigma E}$ for a diffusing medium (case $D$, with $T=5000$, $\Xi=0.25$) is multiplied by white noise of unit root mean square, squared, smoothed, and plotted, $\langle s_t^2 \rangle$, in the dashed line. At late times it decays exponentially. The smoothed square of the repaired $S_t$ is plotted in the pale (red online) solid line. It decays at a late time like a power law $\sim t^{-5/2}$. (b) Comparison of smoothed squared $\partial_t K(t)/2$ (irregular line) with the Sabine $\sigma F(x=0,t)$ (smooth line) for the diffusing medium case $D$, with small $\Xi$. An early time enhancement by a factor of 2 is followed by a later time enhancement that grows to four, slightly greater than the usual quantum echo factor of 3. In accord with the small value of $\Xi$, localization is not strong. (The apparent increase in fluctuation strength at late times is not real, being an artifact of the increasing density of points in the plot.)

$$F(0,t) = (4\pi Dt)^{-1/2}\left[1 + 2\sum_{n=1}^{\infty} \exp(-n^2L^2/Dt)\right], \tag{33}$$

a series that converges best at early times. At sufficiently early times $F=E$.

We consider three cases, all with $L=1$. For each case a Sabine $s_t$ is constructed by $s_t = r_t\,[\sigma E(x=0,t)]^{1/2}$ as was done following Eq. (20). It is then repaired using the methods of Sec. II B. For each case we focus, in particular, on a comparison of the Sabine energy density $\sigma F(0,t)$ and the repaired energy density determined by squaring the inverse Fourier transform of $S(\omega)/[1+S(\omega)]$.

The first, case $D$, illustrated in Figs. 6, is for a small $\Xi$, i.e., an unlocalized system, with $E(t)$ determined from Eqs. (29) and (30) using $T=5\,000$, i.e., $D=2\times10^{-4}$, and $\Xi = 0.25$, i.e., $\sigma = 10^{-4}$.

Figure 7 presents the recapture rates and energy densities for case $E$ having $\Xi=1.0$, and $T=30\,000$. In accord with the

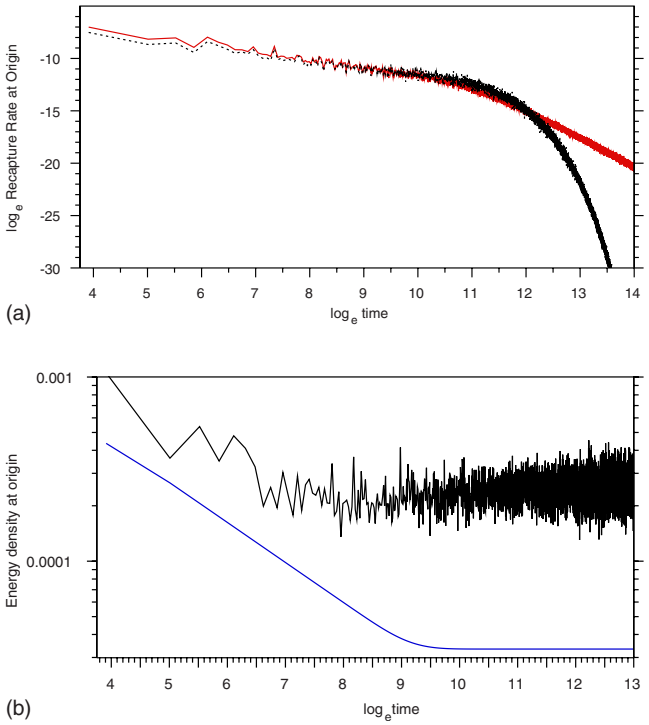


FIG. 7. (Color online) (a) The Sabine envelope $\sqrt{\sigma E}$ for a diffusing medium (case $E$, with $T=30\,000$, $\Xi=1.0$) is multiplied by white noise of unit root mean square, squared, smoothed, and plotted, $\langle s_t^2 \rangle$, in the dashed line. At late times it decays exponentially. The smoothed square of the repaired $S_t$ is plotted in the pale (red online) solid line. It decays at a late time like a power law $\sim t^{-5/2}$. (b) Comparison of smoothed squared $\partial_t K(t)/2$ (irregular line) with the Sabine $\sigma F(x=0,t)$ (smooth line) for the diffusing medium case $E$, with moderate $\Xi$. An early time enhancement by a factor of 2 is followed by a later time enhancement that grows to 8. This indicates, after considering the quantum echo, which accounts for a factor of 3, a degree of localization consistent with a moderate value of $\Xi$.

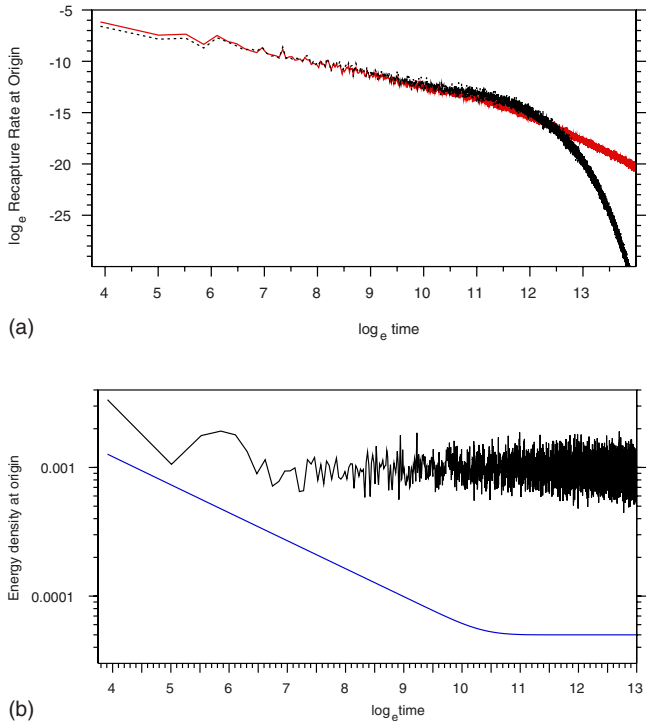


FIG. 8. (Color online) (a) The recapture rates for case $F$ with $T=100\,000$ and $\Xi=5.0$. Again $\langle S^2 \rangle$ [pale solid curve (red online)] exhibits an enhanced backscatter factor of 2 at early times. As in Figs. 6(a) and 6(b), it also reproduces much of the fluctuations in the original $\langle s^2 \rangle$ and shows a power law tail. (b) In case $F$ with its larger value of $\Xi$ (=5), $(\partial_t G^0)^2$ (irregular line) shows an asymptotic enhancement by a factor of about 18 over the Sabine prediction (smooth curve).

larger value of $\Xi$, late time enhancements in Fig. 7(b) are stronger than they were in Fig. 6(b).

Figures 8 and 9 show the recapture rates and energy densities from the cases $(F)$ and $(G)$ for which $\Xi=5$, $T=100\,000$ and $\Xi=10$, $T=100\,000$, respectively. The degree of enhancement continues to increase with $\Xi$, consistent with a decreasing localization length.

## V. CONCLUSIONS

There should perhaps be no surprise that the procedure here yields Wigner reaction matrices $\mathsf{K}$ and Green's functions $G^0$ that show localization. The recipe embodies the Thouless criterion that localization is due to the time scale for resolving levels (i.e., modal density, Heisenberg time, recapture) being short compared to transport time scales. If most probability is recaptured before much transport has transpired, then $S(t)$ contains no record of transport. If a structure is such that most trajectories beginning at the incoming channel escape back through that channel before exploring the entire structure, then the reflection $S(t)$ contains no record of transport. But responses $\mathsf{K}$ and $G^0$ in the corresponding closed system are merely concatenations of $\mathsf{S}$ [Eq. (10)], so they also will have little signature of transport. This picture, with its emphasis on the role of backscatter, is reminiscent of weak-localization arguments [20] for the onset of full Anderson localization. It differs, however, in that the present approach applies in principle to systems lacking time-reversal invariance, unlike the argument of Vollhardt and Wolfle [20]. It will be interesting to see how the evolutions of energy density determined by this approach compare with those from the self-consistent theory of transport in localizing systems [21,22].

While theory with which to better understand these behaviors is needed, there is also room for further numerical experiments. One wonders, in particular, how these results might be modified if the assumption of prompt transmission were relaxed, or if other short time features were included in $s$. Level statistics could be examined also. Finally, the recipe ought to be extended to $S$ matrices with rank $M$ greater than one. Such an extension would greatly expand the applicability of $s$-matrix unitarization.

## ACKNOWLEDGMENTS

The author thanks numerous people for stimulating discussions, in particular, Yan Fyodorov, Thomas Seligman, and

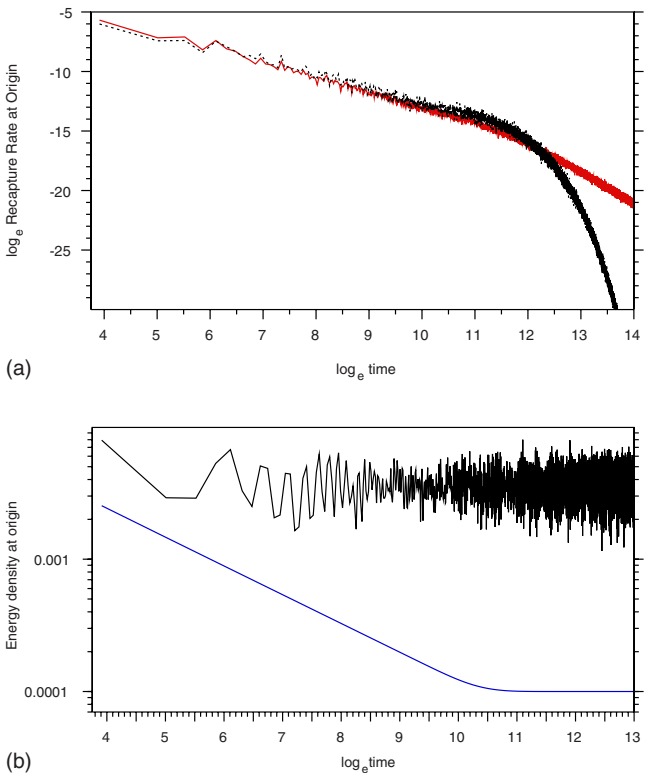


FIG. 9. (Color online) (a) The recapture rates for case $G$ with $T=100\,000$ and $\Xi=10.0$. The Sabine $\langle s_t^2\rangle$ is given by the dashed line; the repaired $\langle S_t^2\rangle$ is given by the solid line. (b) At the largest value of $\Xi$ considered (case $G$, $\Xi=10$) the energy at late times in $(\partial_t G^0)^2$ (irregular line) is about 35 times greater than that predicted by Sabine (smooth line).

Olivier Legrand. He thanks the University of Nice where much of this work was done. Computational resources were provided by the NCSA. The work was supported also by the National Science Foundation, Grant No. CMS-0528096.

## APPENDIX: EVALUATION OF THE $\chi$

The $S$ matrices generated in Secs. III and IV correspond to 100% prompt transmissions, as may be seen in that they lack any prompt reflections. They have no delta-function character at time zero. The corresponding $\mathsf{K}$'s were constructed from Eq. (10). $K$ is in turn related to the response of the undamped reverberant system $G^0$ by means of Eq. (8). To construct $G^0$ (or rather its matrix element $v^T G^0 v$, which is the most one could hope to get from $\mathsf{K}$) and from that construct the corresponding evolution of energy density at $\{v\}$ in the undamped isolated system, we need to know the $\chi$.

As the $S$ have negligible contributions at time zero, $\mathsf{K}$ near time zero will be, by Eq. (10), merely the identity times a step function, $\mathsf{I}\Theta(t)$. Thus, for short times $t$,

$$\partial_t \mathsf{K}_{ab} = \mathsf{I}\delta_{ab}\delta(t) = \{v_a\}^T[\partial_t G^0(t)]\{v_b\}\sqrt{\chi_a\chi_b}, \tag{A1}$$

which relates the early time behavior of $[G^0]$ to the $\chi$.

$[G^0]$ is given also in terms of the eigenvectors of $[H]$ by

$$[G^0(t)] = \sum_r \{u^r\}\{u^r\}^T \sin \omega_r t/\omega_r, \quad \text{where } [H]\{u^r\} = \omega_r^2\{u^r\}. \tag{A2}$$

$G^0$'s time derivative evaluated at the diagonal element $(bb)$, while noting that $u_b^r \equiv \{v_b\}^T\{u^{(r)}\}$ has an expected square value of $1/N$, is

$$\partial_t G^0_{bb}(t) = \partial_t\{v_b\}^T[G^0]\{v_b\} = \sum_r (u_b^r)^2 \cos \omega_r t$$

$$= (1/N)\int_0^\Omega n(\omega_r)\cos \omega_r t d\omega_r. \tag{A3}$$

For the uniform modal density $n(\omega)$, which we consider here, $n$ is given by $N/\Omega = T_H$, where $\Omega$ is the total bandwidth covered by the natural frequencies. Thus

$$\partial_t G^0_{aa}(t) = (1/\Omega)\int_0^\Omega \cos \omega_r t \, d\omega_r = (\sin \Omega t/\Omega t). \tag{A4}$$

When integrated over a short time interval near zero (less than the time scale for transport dynamics and reverberation, but greater than the inverse bandwidth) this becomes $\pi/2\Omega$. Thus we identify, for short times,

$$\partial_t G^0_{aa}(t) = \pi\delta(t)/2\Omega, \tag{A5}$$

and

$$\sqrt{\chi_a^2} = 2\Omega/\pi. \tag{A6}$$

This is equivalent to the expression for $\kappa_a$ given by Fyodorov *et al.* [[2], Eq. (5)] for the random matrix Schrödinger equation.

For the cases discussed in Secs. III and IV, the spectrum is uniformly distributed from frequency $f=0$ to the Nyquist frequency of $1/2$. Inasmuch as the spacing in time $\delta t$ is unity, the Nyquist frequency $f_{\text{Nyquist}}$ is $1/2$, and the natural circular frequencies $\omega_r$ lie between zero and $2\pi f_{\text{Nyquist}}$. Thus $\Omega=\pi$ and $\chi=2$.

The reverberant part of $G$ is the second term of Eq. (7), and may be compared with Sabine-type predictions $\sigma F(t)$. Half the square of $\partial_t G^0(t)$ is the kinetic energy density. The total energy density includes potential energy and is twice this. Thus in Figs. 2–9 we compare

$$[\partial_t G^0(t)]^2 = [\partial_t K(t)/2]^2$$

$$= (\text{inverse Fourier transform of } S(\omega)/[1+S(\omega)])^2$$

with $\sigma F(t)$.

[1] Thomas Guhr, Axel Muller-Groeling, and H. A. Weidnemuller, Phys. Rep. **299**, 189 (1998).
[2] Y. V. Fyodorov, D. V. Savin, and H.-J. Sommers J. Phys. A **38**, 10731 (2005).
[3] Oleg Lobkis, Igor Rozhkov, and Richard Weaver, Phys. Rev. Lett. **91**, 194101 (2003).
[4] R. H. Lyon and R. G. DeJong, *Theory and Application of Statistical Energy Analysis* (Butterworths-Heimann, Boston, MA, 1995).
[5] R. S. Langley and P. G. Bremner, J. Acoust. Soc. Am. **105**, 1657 (1999).
[6] M. L. Lai and A. Soom, J. Vibr. Acoust. **112**, 127 (1990).
[7] P. Morse and R. Bolt, Rev. Mod. Phys. **16**, 69 (1944).
[8] Lothar Cremer and Helmut A. Müller, J. Acoust. Soc. Am. **76**, 1277 (1984).
[9] *Diffuse Waves in Complex Media*, NATO ASI, Ser. C., edited by J.-P. Fouque (Kluwer Academic, Dordrecht, 1999), Vol. 531.
[10] Richard L. Weaver and Oleg I. Lobkis, Geophysics **71**, S15 (2006).
[11] R. L. Weaver and W. Sachse, J. Acoust. Soc. Am. **97**, 2094 (1995).
[12] Richard L. Weaver, New J. Phys. **9**, 8 (2007).
[13] J. P. Keating and S. Müller, Proc. R. Soc. London, Ser. A **463**, 3241 (2007).
[14] Richard L. Weaver and Oleg I. Lobkis, J. Sound Vib. **231**, 1111 (2000).
[15] C. Dembowski, H.-D. Gräf, R. Hofferbert, H. Rehfeld, A. Richter, and T. Weiland, Phys. Rev. E **60**, 3942 (1999).
[16] U. Kuhl, H.-J. Stockmann, and R. Weaver, J. Phys. A **38**, 10433 (2005).
[17] The restriction to minimum phase has an interpretation based on Robinson's energy delay theorem, which says that the energy $\Sigma_{t=0}^{T} s_t^2$ summed to any time $T$ is no less for a minimum phase function $s_t$ than for any other causal function with the same spectrum $|s(\omega)|$. The theorem for the more general matrix case may be seen in Y. Inouye, IEEE Trans. Circuits Syst. **34**, 188 (1987).
[18] A. H. Sayed and T. Kailath, Numer. Linear Algebra Appl. **8**, 467 (2001).
[19] V. N. Prigodin, B. Altshuler, K. B. Efetov, and S. Ida, Phys. Rev. Lett. **72**, 546 (1994).
[20] D. Vollhardt and P. Wolfle, Phys. Rev. Lett. **45**, 842 (1980); Phys. Rev. B **22**, 4666 (1980); D. Vollhardt and P. Wolfle, in *Electronic Phase Transitions*, edited by W. Hanke and Yu. V. Kopaev (Elsevier, Amsterdam, 1992).
[21] B. A. van Tiggelen, A. Lagendijk, and D. S. Wiersma, Phys. Rev. Lett. **84**, 4333 (2000); S. E. Skipetrov and B. A. van Tiggelen, *ibid.* **92**, 113901 (2004); **96**, 043902 (2006).
[22] O. I. Lobkis and R. L. Weaver, Phys. Rev. E **71**, 011112 (2005).